Density Functional Theory Study of Hydrogen Bonding in Ionic Molecular Materials

Nicole A. Benedek,[†,‡] Kay Latham,[‡] Ian K. Snook,[†] and Irene Yarovsky*[,†]

Departments of Applied Physics and Applied Chemistry, RMIT University, GPO Box 2476V, Melbourne 3001, Australia

Received: April 10, 2006; In Final Form: May 22, 2006

Crystal structures are usually described in geometric terms. However, it is the energetics of intermolecular interactions that determine the chemical and physical properties of molecular materials.[1] In this paper, we use density functional theory (DFT) in combination with numerical basis sets to analyze the hydrogen bonding interactions in a family of novel ionic molecular materials. We find that the calculated binding energies are consistent with those of other ionic hydrogen bonded systems. We also examine electron density distributions for the systems of interest to gain insight into the nature of the hydrogen bonding interaction and investigate the effects of different aspects of the crystal field on the geometry of the hydrogen bond.

1. Introduction

The discovery of electrically conductive polymers[2,3] in the early 1970s sparked an explosion of interest in the properties of molecular materials. Semiconducting materials consisting of small organic molecules are promising candidates for optoelectronic devices and have thus been the subject of numerous theoretical[4−6] and experimental[7,8] studies. In contrast to their more conventional organic counterparts, inorganic molecular materials may contain any element. A far more diverse range of intra- and intermolecular interactions is therefore possible. Many inorganic molecules are charged, and hence also have counterions in condensed phases. This has consequences for the diversity of interactions, the energies associated with them, and the material properties.[1]

An interesting family of novel ionic molecular crystals, mixed inorganic/organic phosphonates, was recently synthesized and characterized.[9] These layered materials contain a copper ion (Cu^{2+}, d^9) coordinated to two phenanthroline ligands and a halogen substituent, either Cl^-, Br^-, I^-, or NCS^-. The positively charged copper−halogen ions are interleaved between parallel sheets of negatively charged, hydrogen-bonded phenylphosphonic acid dimers, which act as counterions. There are no covalent bonds between individual molecules, either within a layer or between layers. The compounds crystallize in a monoclinic space group, *C*2/*c*, and have their Cu−X bond lying along a 2-fold crystallographic axis. The molecular unit of the iodo form is shown in Figure 1, and a 1 × 2 × 1 supercell is shown in Figure 2.

Our interest in these materials stems from the desire to better understand the complex interactions often present in hybrid organic/inorganic molecular materials. The properties of molecular solids are dictated by features of both molecular and condensed matter physics: their physical properties depend on their crystalline structure, which in turn is governed by interactions between molecules. The diverse range of elements and bonding scenarios in organophosphonate molecular materials means they provide interesting "laboratories" for the study of intermolecular interactions.

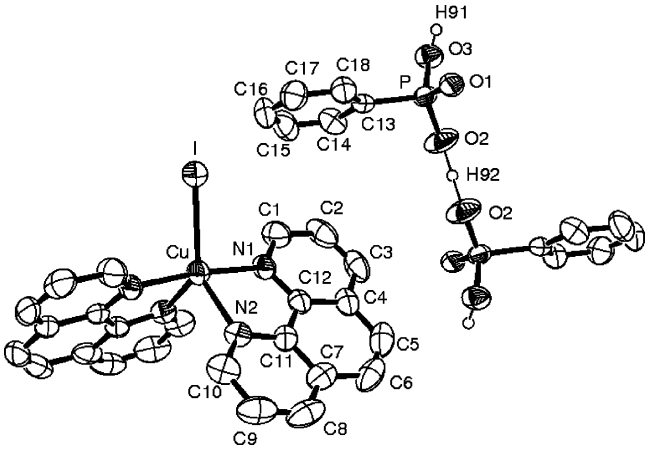

Figure 1. ORTEP perspective of the molecular unit of the iodo form, $[Cu(C_{12}H_8N_2)_2I][(OH)_2OPC_6H_5][(OH)O_2PC_6H_5]$.

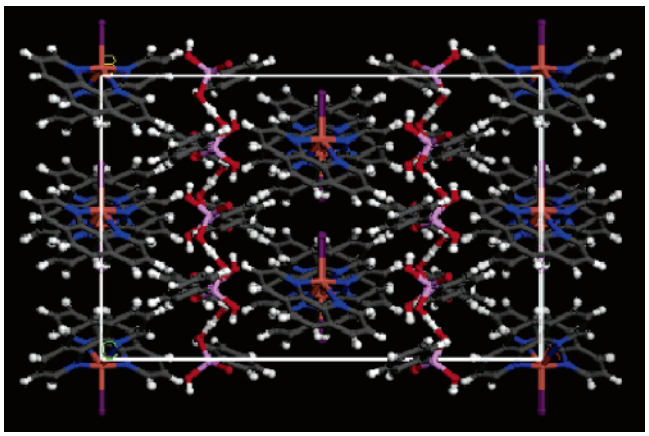

Figure 2. A 1×2×1 supercell of the iodo form. Different atoms are distinguished by the following colors: gray, carbon; white, hydrogen; blue, nitrogen; orange-, copper; dark purple, iodine; light purple, phosphorus; red, oxygen. The same atom coloring scheme has been used for all figures.

In this paper, we use theoretical methods to study both the geometry and energetics of the hydrogen bonding interaction between phenylphosphonic acid dimers in the organophosphonate molecular materials. The phenylphosphonic acid dimers

* Corresponding author. E-mail: irene.yarovsky@rmit.edu.au.
† Department of Applied Physics.
‡ Department of Applied Chemistry.

10.1021/jp062239t CCC: $33.50
Published on Web 09/12/2006

are actually anions formed from the interaction between phenylphosphonic acid and a phenylphosphonate anion. The resulting hydrogen bond is thus ionic. Like the conventional hydrogen bond, ionic hydrogen bonds are involved in a broad range of phenomena: in ionic clusters and nucleation, in the structures of ionic crystals, surfaces, silicates and clays, and in self-assembly in supramolecular chemistry and molecular crystals. They are also important in biological processes, such as protein folding, formation of membranes, and biomolecular recognition. A fundamental understanding of the properties of ionic hydrogen bonds is thus vital to the understanding of many different phenomena.

The primary interaction in the phenylphosphonic acid dimers is an $O-H-O^-$ bond; it is therefore an example of a symmetric ionic hydrogen bond—one in which the proton donor and acceptor are chemically identical. Ionic hydrogen bonds are typically characterized by short bond lengths and strong binding energies in the range of $-(5-35)$ kcal/mol.[10] Anionic $O-H-O^-$ interactions are no exception with bond lengths in the range of 2.4−2.5 Å and binding energies of about −28 kcal/mol.[11−13] As a point of comparison, the O−O distance in water dimer, classified as a neutral moderate hydrogen bond, is 2.976 Å with a binding energy of about −5 kcal/mol. Short hydrogen bonds, such as $O-H-O^-$ bonds, are usually centrosymmetric, which means that the proton is drawn to the midpoint of the O−O axis and therefore can no longer be associated with either a donor or acceptor. This has implications for the theoretical treatment of such bonds.

The phenylphosphonic acid dimers are large molecules. We therefore need both accurate and efficient basis sets for our hydrogen bonding study. We recently investigated and compared the ability of Gaussian-type and numerical basis sets to accurately describe both the geometries and binding energies of a selection of hydrogen bonded systems.[14] We found that both types of basis set produced comparably accurate results; however, the numerical basis sets were found to be at least 10 times faster than the Gaussian-type basis sets. In this paper, we apply the findings of this previous investigation to our study of hydrogen bonding interactions in organophosphonate molecular materials.

This paper is organized as follows: in section 2 we discuss the parameters used in our calculations. We calculate the binding energies of our model systems in section 3.1 and consider the effect of substituents on the strength and geometry of the hydrogen bonding interaction in section 3.2. In section 3.3, we aim to understand, and possibly quantify, the effect of the crystal field on the structure of the phenylphosphonic acid molecules in the organophosphonates. We draw our conclusions in section 4.

2. Computational Details

Experimental data on the energies associated with particular interactions in molecular materials are scarce, mostly due to the difficulty involved in carrying out such experiments. Hence, computational simulations are an important complement to experimental techniques in probing the electronic structure of complex materials.

In section 1, we noted that each member of the materials family studied here contains chains of phenylphosphonic acid molecules linked by single, linear hydrogen bonds to form dimers. These negatively charged dimers form two hydrogen bonds with each other to form chains along the *b* axis of the crystal. There are also dispersion interactions between the aromatic rings of dimers in adjacent chains to form sheets. A fragment of one of these sheets is shown in Figure 3. We have thus simulated phenylphosphonic acid dimer in two different hydrogen bonding scenarios to represent the two arrangements present in the molecular crystal: a negatively charged (−1) dimer linked by a single, linear hydrogen bond and a neutral dimer of acid molecules linked by two hydrogen bonds, as shown in Figure 4. The initial coordinates for each structure were obtained from the bulk crystal, the structure of which was determined by single-crystal X-ray diffraction.[9] The geometries of each model system were optimized, without constraints, and the binding energy was calculated as follows:

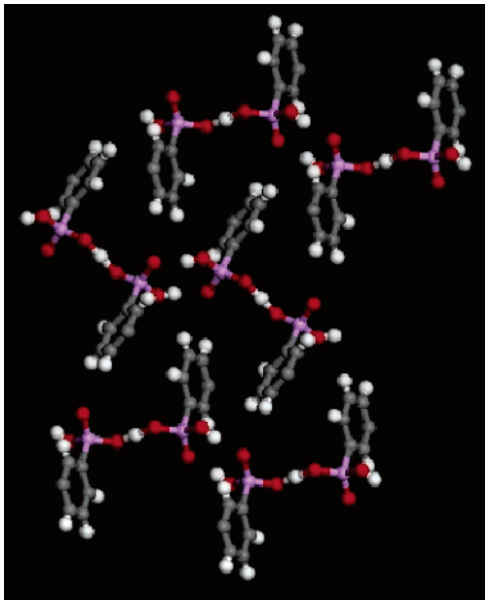

Figure 3. Hydrogen bonding interactions between phenylphosphonic acid dimers.

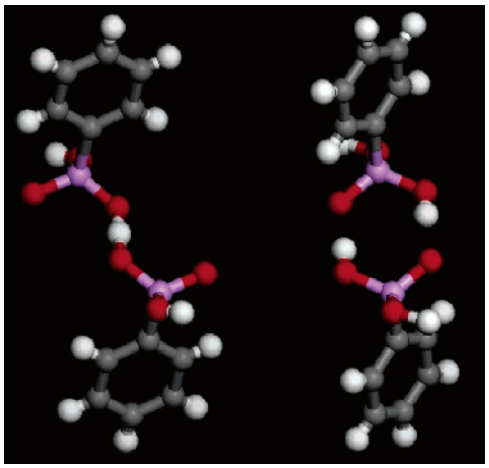

Figure 4. Phenylphosphonic acid dimer model systems. Left: single, linear H-bonded dimer (charge −1). Right: double H-bonded dimer (charge neutral).

$$\Delta E = E_{AB} - (E_A + E_B)$$

where E_{AB} is the total energy of the relaxed dimer and E_A and E_B are the total energies of the relaxed constituent fragments. All calculations are all-electron and spin-restricted, unless otherwise stated. The symmetries of each model considered were either C_i or C_1; hence, we have not used symmetry in our calculations.

One conclusion from our numerical basis set study[14] was that the PBE functional performed very well for geometries but had

a tendency to overbind. In contrast, the HCTH and BLYP functionals performed less well for geometries but produced more accurate energies. These trends were reflected in the results for phosphinic acid dimer, the test system which most closely resembles phenylphosphonic acid dimer. Since the only experimental information available for phenylphosphonic acid dimer is the geometric parameters, it would make sense to choose a functional on the basis of its ability to accurately predict geometries. Hence, the geometry of each model system has been optimized and the binding energy calculated with the PBE functional in combination with the DNP numerical basis set (double numerical plus polarization). We have assumed, on the basis of the data for phosphinic acid dimer, that PBE will produce a lower binding energy (too strong binding) for phenylphosphonic acid dimer than the HCTH or BLYP functionals. To test this assumption, we have also performed single-point energy calculations using the HCTH functional on the PBE-optimized geometry for the single H-bond dimer only.

No ionic hydrogen-bonded dimers were included in the numerical basis set study. To confirm the reliability of the numerical basis sets for these systems, we have also calculated the binding energy of the single H-bond dimer using the PBE functional in combination with the Gaussian-type 6-31+G(d,p) basis set. All of our calculations have been performed with the Gaussian03[15] (Gaussian-type basis sets) and DMol^3 (refs 16 and 17, numerical basis sets) codes. Counterpoise corrections were not performed; this procedure is not implemented in DMol^3. However, the use of numerical basis sets greatly minimizes and perhaps even eliminates the basis set superposition error.[16]

3. Results and Discussion

3.1. Relaxations and Binding Energy. Unsubstituted Dimers. The energy of hydrogen bonds in the solid state cannot be directly measured. However, computer simulations allow us to isolate these interactions and study them quantitatively in the gas phase. Geometry and continuum effects tend to decrease the strengths of ionic hydrogen bonds in solids,[10] so gas-phase binding energies provide an upper limit to the bond strength.

The binding energy for the optimized single H-bond arrangement was calculated to be −27.1 kcal/mol with the PBE functional and DNP basis and −26.4 kcal/mol with the PBE functional and 6-31+G(d,p) Gaussian-type basis, thus confirming the suitability of the numerical basis sets to describe ionic hydrogen-bonded systems. An additional calculation on the PBE-optimized geometry with the HCTH functional and DNP basis yielded a binding energy of −23.6 kcal/mol, which suggests that the energies obtained with the PBE functional are slightly overestimated. All energies obtained are consistent with those calculated for phosphinic acid dimer and for the other $(HOH\cdots OH)^-$ systems, described earlier.[10−13]

The geometry of the PBE-optimized structure is in excellent agreement with the experimental one, as shown in Table 1. The biggest discrepancy concerns the C−P−O−H torsion angle, which is larger in the experimental structure than the optimized one and is probably due to compression effects in the crystal. Crystal field effects will be discussed in more detail in section 3.3.

We have also performed calculations on the uncharged double H-bond dimer. The main geometric parameters for both the optimized (PBE functional and DNP basis set) and experimental structure are compared in Table 1. The binding energy of the relaxed structure is predicted to be −22.8 kcal/mol, slightly weaker than that obtained for the single H-bond dimer, as expected because the double H-bond dimer is not charged.

TABLE 1: Comparison of Main Geometric Parameters between Experimental and Optimized (PBE/DNP) Structures for H-Bonded Dimers Considered in This Work

	experiment	optimized
Single H-Bond Dimer		
d(O···O), Å	2.426	2.414
d(O···H), Å	1.213	1.207
O−H−O, deg	180	180
C−P−O−H, deg	82	63
Double H-Bond Dimer		
d(O···O), Å	2.517	2.572
d(O···H), Å	1.724	1.546
O−H−O, deg	175	175
C−P−O−H, deg	103	96
Nitro-Substituted Dimer		
d(O···O), Å	2.433	2.422
d(O···H), Å	1.498	1.154
d(H···O′), Å	0.943	1.268
O−H−O, deg	171	179
C−P−O−H, deg	75	60
C′−P′−O′−H′, deg	79	58
Methyl-Substituted Dimer		
d(O···O), Å	2.410	2.415
d(O···H), Å	1.208	1.208
O−H−O, deg	180	180
C−P−O−H, deg	88	76

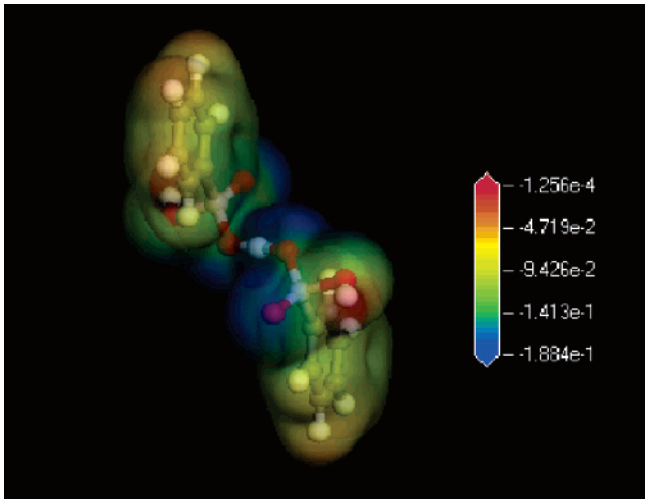

Figure 5. Electrostatic potential mapped onto the electron density calculated at the PBE/DNP level of theory for the single H-bond dimer (unsubsituted).

Insight into the nature of the hydrogen bonding interaction between phenylphosphonic acid molecules may be obtained by examining the electron density map of the single H-bond dimer, Figure 5. Less negative regions (red) correspond to electron-deficient areas, while highly negative regions (blue) correspond to electron-rich areas. We note that although electron density maps are quantitatively calculated, their real value lies in their use as a tool to qualitatively compare the electron distributions in chemically different structures.

Figure 5 shows that much of the electron density is concentrated in and around the hydrogen bond which links the phenylphosphonic acid and anion molecules. This area contains a number of oxygen atoms, which pull electron density out of the aromatic rings thereby leaving them electron-deficient. Addition of a second dimer to form a chain fragment does little to alter this behavior, as shown in Figure 6. The hydrogen bonds linking the phenylphosphonic acid molecules form an electron-rich "spine", which runs along the *b* axis of the crystal.

3.2. Relaxations and Binding Energy. Substituted Dimers. A second series of mixed-ligand copper organophosphonate

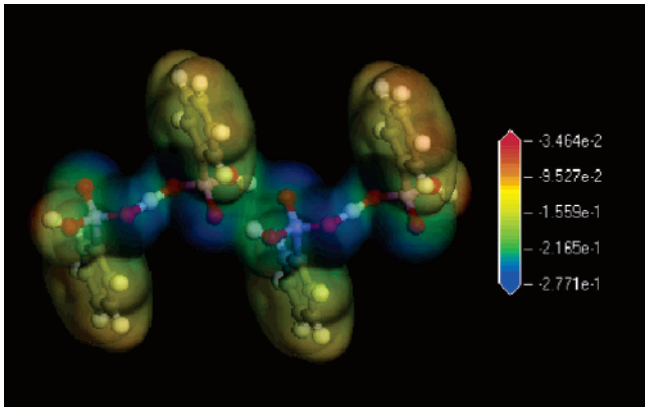

Figure 6. Electrostatic potential mapped onto the electron density calculated at the PBE/DNP level of theory for two single H-bond dimers. The total charge of this model is −2.

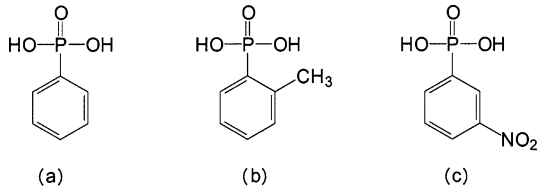

Figure 7. Acid fragments of the hydrogen-bonded dimer anions considered in this work: (a) unsubstituted phenylphosphonic acid; (b) *o*-methylphenylphosphonic acid; (c) *m*-nitrophenylphosphonic acid.

TABLE 2: Comparison of the Main Geometric Parameters (Experimental) between the Nitro-Substituted and Unsubstituted Phenylphosphonic Acid Dimers

	nitro-substituted	unsubstituted
d(O···O), Å	2.433	2.426
d(O···H), Å	1.498	1.213
d(H···O′), Å	0.943	1.213
O−H−O, deg	171	180
C−P−O−H, deg	75	82
C′−P′−O′−H′, deg	79	82

materials was recently synthesized.[18] These new compounds are similar to the materials described in section 1, but phenylphosphonic acid was replaced by a substituted phenylphosphonic acid derivative; e.g., the aromatic ring bears either a nitro (NO_2) group or methyl (CH_3) group in place of one hydrogen, as shown in Figure 7. The molecular unit of the new structures is analogous to that of the parent compounds—a five-coordinate $[Cu(phen)_2X]^+$ cation with two acid molecules in some arrangement functioning as a counterion. In this section, we will consider the effects of the nitro and methyl substituents on the geometry and energetics of the hydrogen bonding interaction.

The molecular unit of the nitro-substituted organophosphonate contains an acid and anion molecule linked by a single H-bond; the dimer carries a total charge of −1. The main geometric parameters of the nitro-substituted dimer are compared with those of the unsubstituted parent in Table 2. An immediate observation is that the nitro-substituted dimer is not symmetric; the two torsion angles are inequivalent as are the O···H bond lengths. It follows from the latter observation that the hydrogen bond in the nitro-substituted dimer is not centrosymmetric; i.e., the hydrogen atom can be unambiguously associated with the proton-donating (acid) fragment.

The geometry of the nitro-substituted dimer was optimized in the same manner as that for the unsubstituted dimers, with the PBE functional and DNP basis set. The total charge was set to −1. Table 1 shows that the optimized structure is more symmetric than the experimental one. The O···O distance is shorter in the optimized structure, and the hydrogen atom has been drawn away from the donating acid toward the midpoint of the hydrogen bond, which is considerably more linear (179°) than in the experimental structure (171°). The largest discrepancy between experiment and theory again concerns the C−P−O−H torsion angles. A contraction of the O···O distance and a decrease in C−P−O−H torsion angle was also observed for the unsubstituted single H-bond dimer.

TABLE 3: Comparison of Main Geometric Parameters (Experimental) between the Methyl-Substituted and Unsubstituted Phenylphosphonic Acid Dimers

	methyl-substituted	unsubstituted
d(O···O), Å	2.410	2.426
d(O···H), Å	1.208	1.213
O−H−O, deg	180	180
C−P−O−H, deg	88	82

We have also examined the effect of the substituent on the binding energy of the dimer. Nitro groups are known to be strong electron-withdrawing agents; hence, we might expect the hydrogen bond in the nitro-substituted dimer to be weaker than its unsubstituted analogue. Furthermore, the O··O distance in the nitro-substituted dimer is slightly longer than in the unsubstituted parent, and this also suggests that the hydrogen bond may be weaker. In fact, the binding energy of the nitro-substituted dimer is predicted to be −31.75 kcal/mol, about 5 kcal/mol *stronger* than the unsubstituted single H-bond dimer.

This initially counterintuitive result can be readily explained by considering the dissociation constants (pK_a) of the substituted and nitro-substituted dimers. Nagarajan et al.[19] determined the dissociation constants of 36 substituted phenylphosphonic acids. They found that nitro-substituted phenylphosphonic acid had a significantly lower dissociation constant (1.28) than its unsubstituted parent (1.86). This means that nitro-substituted phenylphosphonic acid is a stronger acid, and we could therefore expect it to form a stronger hydrogen bond. Another possibility is that the stronger binding is merely a result of geometric differences between the substituted and unsubstituted single H-bond dimers. To test this hypothesis, we performed an additional single-point energy calculation on the relaxed nitro-substituted dimer whereby the nitro groups were replaced with hydrogen atoms. The binding energy of this structure was calculated to be −26.69 kcal/mol, similar to that obtained for the unsubstituted single H-bond dimer. Hence, the stronger binding energy of the nitro-substituted dimer must have electronic effects (exerted by the nitro groups) at its origin.

The molecular unit of the methyl-substituted organophosphonate also contains an acid and anion molecule linked by a single H-bond; this dimer also carries a total charge of −1. The structure of the methyl-substituted single H-bond dimer is almost identical to that of its unsubstituted parent, as Table 3 shows. The hydrogen bond linking the two fragments is linear and centrosymmetric. In contrast to both the nitro and unsubstituted dimers, geometry optimization lengthens, rather than shortens, the O···O distance, Table 1. Given the similarity between the methyl-substituted and unsubstituted geometries and the fact that methyl groups are only very weakly electron donating, we might expect the binding energy of the methyl-substituted dimer to be very similar to the unsubstituted single H-bond dimer. This is indeed the case; the binding energy of the methyl-substituted dimer is predicted to be −26.01 kcal/mol. The electron density distribution of the methyl-substituted dimer (not shown) is almost identical to that of the unsubstituted dimer.

3.3. Crystal Field Effects. The crystalline field is the total influence of the crystal surroundings on a target molecule. A

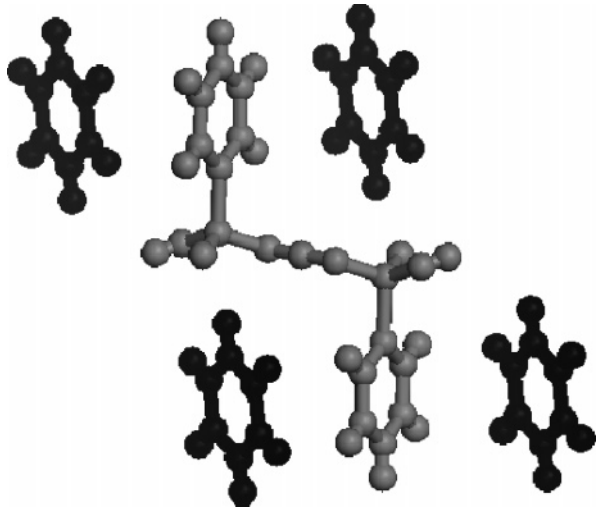

Figure 8. Unsubstituted single H-bond phenylphosphonic acid dimer with aromatic rings from adjacent dimer molecules. Black atoms have been constrained in their experimental positions, while gray atoms have been allowed to relax, without constraints.

large amount of information about molecular structure now comes from the crystal structure. Implicit in these descriptions is the assumption that the crystal environment has not affected bond lengths and therefore the overall structure of the molecule. This hypothesis was originally formulated by the Russian crystallographer Kitaigorodsky,[20] who believed that the major effect of the crystalline field on molecular structure was to compress the molecule and promote favorable stacking by distorting torsion angles. However, in recent studies[21,22] of crystal structures containing metal complexes, it was found that the crystalline field can indeed significantly affect bond lengths. Let us then examine the hydrogen bonding interaction between the unsubstituted phenylphosphonic acid dimers in light of Kitaigorodsky's hypothesis.

In sections 3.1 and 3.2 we saw how geometry optimization of the single H-bonded dimers tended to decrease C−P−O−H torsion angles and shorten O···O distances. The optimizations were performed in the gas phase; i.e., the dimers were modeled in complete isolation from the crystal environment. Hence, it is pertinent to ask, which features of the crystal environment are responsible for the observed experimental geometries of the single H-bonded dimers?

Figure 3 shows that, in addition to hydrogen bonding interactions between dimers to form chains, there are also dispersion interactions between the aromatic rings of the dimers to form an acid "sheet". As a first step, let us assume that the discrepancies between the experimental and optimized structures are caused by a failure to account for these aromatic ring interactions. Interactions between aromatic rings are very weak; hence, the rings probably represent more of a steric, rather than chemical constraint. To test our assumption, we have constructed a model of the unsubstituted single H-bond dimer in which the aromatic rings of adjacent dimers have been included, as shown in Figure 8. The aromatic rings of the adjacent dimers were constrained in their experimental positions, while the single H-bond dimer was allowed to relax, without constraints. The total charge was set to −1. In this model, the O···O distance still shortens to 2.417 Å but the C−P−O−H angle only decreases to 75°, in better agreement with the experimentally observed angle of 82°. Hence, steric constraints imposed by the aromatic rings are not alone responsible for the experimentally observed geometry.

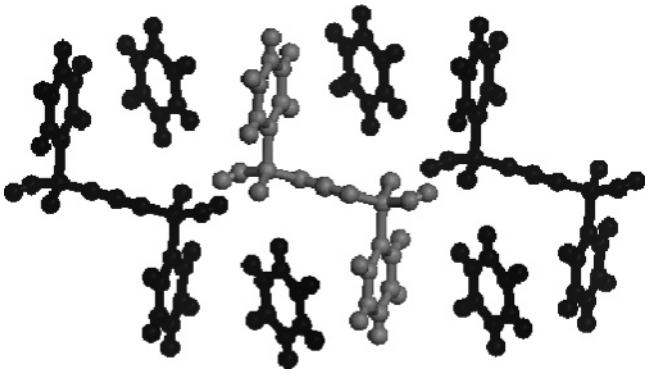

Figure 9. Unsubstituted single H-bond phenylphosphonic acid dimer with aromatic rings from adjacent dimer molecules and hydrogen bonding dimers. Black atoms have been constrained in their experimental positions, while gray atoms have been allowed to relax, without constraints.

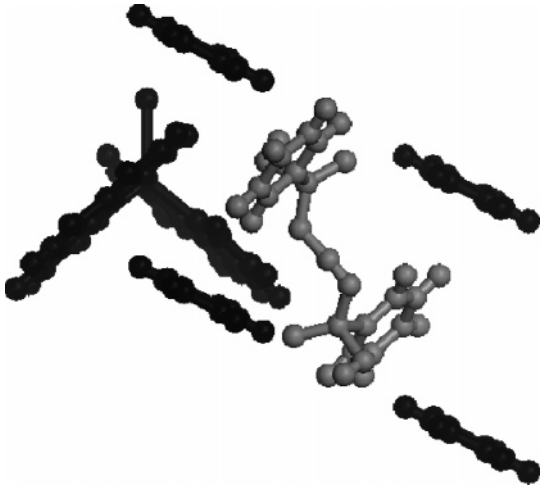

Figure 10. Unsubstituted single H-bond phenylphosphonic acid dimer with aromatic rings from adjacent dimer molecules and copper−halogen cation. Black atoms have been constrained in their experimental positions, while gray atoms have been allowed to relax, without constraints.

We have made repeated mention of the hydrogen bonding interaction between dimers to form chains. These hydrogen bonds could be considered as chemical rather than steric constraints. It would thus be sensible to construct a model in which these interactions are included. Hence, in addition to the aromatic rings of adjacent dimers, we have added two single H-bond dimers which form hydrogen bonds with our target dimer, as shown in Figure 9. Once again, all molecules except for the target dimer were constrained in their experimental positions while the target dimer was allowed to relax, without constraints. In this model, the O···O distance still contracts to 2.418 Å, but the C−P−O−H angle *increases* to 110°. Steric constraints together with chemical constraints imposed by the hydrogen bonding interaction are still not sufficient to reproduce the experimentally observed geometry. Furthermore, a possible problem with this model is that it carries a large negative charge of −3 (each dimer unit carries a charge of −1). In the crystal, the phenylphosphonic acid dimer anions are charge-balanced by the copper−halogen cations, which carry a charge of +1.

In the final model for this section, we include the charge-balancing cation in addition to the aromatic rings of adjacent dimers, as shown in Figure 10. An ideal model would also include the hydrogen bonding interactions included in the previous model; however, to maintain charge neutrality, this would require the addition of two extra cations to the current

model, i.e., three phenylphosphonic acid anions balanced by three copper−halogen cations. Calculations on such a model were attempted but proved too computationally expensive. All calculations on the present model (Figure 10) were performed using the "All Electron Relativistic" option available in DMol[3], which includes all electrons explicitly and introduces some relativistic effects into the core. The model was charge neutral; however, an unpaired spin was associated with the Cu^{2+} center. The calculations were therefore spin-unrestricted.

The copper−halogen cation and aromatic rings have been constrained while the target dimer was allowed to relax. In contrast to the previous two models, the O···O distance increases to 2.475 Å. The C−P−O−H angle also increases to 94°. It is tempting to conclude that electrostatic forces induced by the copper−halogen cation act to lengthen the O···O distance. However, the model shown in Figure 9 also contains electrostatic interactions—in the form of hydrogen bonding anions—and no such lengthening is observed. Hence, it is more likely that the presence of an unpaired electron (associated with the Cu^{2+} cation) in the current model is responsible for the observed lengthening. This hypothesis is supported by masNMR data (unpublished), which show an interaction between the phosphorus atoms of the anion and the copper center.

The C−P−O−H torsion angle appears to be most sensitive to crystal field effects, in agreement with Kitaigorodsky's hypothesis. In a recent study[21] of the effects of the crystal field on crystal structures containing metal complexes, torsion angles showed deviations of up to 47°. The O···O bond length also appears to be affected by the crystal environment, in apparent contradiction of Kitaigorodsky's hypothesis but in support of the findings of recent studies.[21,22] The discrepancies between experiment and theory in each model considered were less than 0.01 Å; however, this is still larger than the uncertainty in the X-ray structure (by about 1 order of magnitude). Overall, the results of this section suggest that the observed experimental geometry of the single H-bond dimer is a complex product of competing intra- and intermolecular forces and crystal field effects.

4. Summary

We have calculated the binding energies and geometries of substituted and unsubstituted phenylphosphonic acid dimers in a family of novel ionic molecular crystals. We also considered the effect of various parts of the crystal field on the geometry of a single, unsubstituted phenylphosphonic acid dimer anion.

The optimized geometries of each dimer system studied were in good agreement with the experimentally determined geometries, and the calculated binding energies were also consistent with those of other ionic hydrogen bonded systems. The calculational methodology is thus appropriate for these systems. The binding energy of the methyl-substituted dimer was close to that of its unsubstituted parent, as expected given the similarity between the structures of the two dimers and their respective electron density distributions. The nitro-substituted dimer was found to have a lower binding energy (stronger binding) than both the methyl-substituted and unsubstituted dimers. The crystal packing arrangements for each of the three different dimers are similar. We are thus tempted to conclude that the structure is robust to changes in the phenylphosphonic acid. However, it is unclear whether differences in crystal packing are caused by the identity of the substituent or merely its position on the aromatic ring (ortho-, meta-, or para-). The work of Nagarajan et al.[19] appears to suggest that the identity of the substituent is not as important as its position on the ring. Further studies are currently underway to address this issue.

The C−P−O−H torsion angle was found to be the most sensitive geometric parameter to crystal field effects, in agreement with Kitaigorodsky's hypothesis. We adopted a cluster model approach which allowed us to selectively "switch on" different parts of the crystal field interaction and to see the effect of each part on the geometry of the anion. When the dimer was simulated in isolation, the O···O distance contracted and this did not change with the inclusion of hydrogen bonding interactions. In contrast, the inclusion of the cation and the unpaired electron associated with it, increased the O···O distance. Larger, more sophisticated models may shed more light on this important problem.

Acknowledgment. N.A.B. acknowledges the financial support of an Australian Postgraduate Award (APA) and a grant of computer time from the Australian Partnership for Advanced Computing (APAC).

References and Notes

(1) Dance, I. *CrystEngComm* **2003**, *5*, 208.
(2) Chiang, C. K.; Fincher, C. R.; Park, Y. W.; Heeger, A. J.; Shirakawa, H.; Louis, E. J.; Gau, S. C.; MacDiarmid, A. G. *Phys. Rev. Lett.* **1977**, *39*, 1098.
(3) Shirakawa, H.; Louis, E. J.; MacDiarmid, A. G.; Chiang, C. K.; Heeger, A. J. *J. Chem. Soc., Chem. Commun.* **1977**, *16*, 578.
(4) Hummer, K.; Puschnig, P.; Ambrosch-Draxl, C. *Phys. Rev. B* **2003**, *67*, 184105.
(5) Hummer, K.; Puschnig, P.; Ambrosch-Draxl, C. *Phys. Rev. B* **2004**, *92*, 147402.
(6) Hummer, K.; Puschnig, P.; Ambrosch-Draxl, C. *Phys. Rev. B* **2005**, *71*, 081202.
(7) Aust, R. B.; Bentley, W. H.; Drickamer, H. G. *J. Chem. Phys.* **1964**, *41*, 1856.
(8) Oehzelt, M.; Resel, R.; Nakayama, A. *Phys. Rev. B* **2002**, *66*, 174104.
(9) Clarke, R.; Latham, K.; Rix, C.; Hobday, M.; White, J. *CrystEngComm* **2005**, *7*, 28.
(10) Meot-Ner, M. *Chem. Rev.* **2005**, *105*, 213.
(11) Gronert, G. *J. Am. Chem. Soc.* **1993**, *115*, 10258.
(12) Pliego, J. R.; Riveros, J. M. *J. Chem. Phys.* **2000**, *112*, 4045.
(13) Lee, H. M.; Tarkeshwar, P.; Kim, K. S. *J. Chem. Phys.* **2004**, *121*, 4657.
(14) Benedek, N. A.; Snook, I. K.; Latham, K.; Yarovsky, I. *J. Chem. Phys.* **2005**, *122*, 144102.
(15) Frisch, M. J.; et al. *Gaussian03*; Gaussian, Inc.: Pittsburgh, PA, 2003.
(16) Delley, B. *J. Chem. Phys.* **1990**, *92*, 508.
(17) Delley, B. *J. Chem. Phys.* **2000**, *113*, 7756.
(18) Latham, K.; Coyle, A. M.; Rix, C. J.; Fowless, A.; White, J. M. *Polyhedron*, in press.
(19) Nagarajan, K.; Shelly, K. P.; Perkins, R. R.; Stewart, R. *Can. J. Chem.* **1987**, *65*, 1729.
(20) Kitaigorodsky, A. I. *Molecular Crystals and Molecules*; Academic Press: New York, 1973.
(21) Martin, A.; Orpen, A. G. *J. Am. Chem. Soc.* **1996**, *118*, 1464.
(22) Ali, B.; Dance, I.; Scudder, M.; Craig, D. *Cryst. Growth Des.* **2002**, *2*, 601.